Effective Material Modeling for Laminated Iron Cores With a T, Φ-Φ Formulation

Valentin Hanser, Markus Schöbinger, and Karl Hollaus

Institute of Analysis and Scientific Computing, TU Wien, 1040 Vienna, Austria

In the effective medium theory, a material parameter of a heterogeneous structure is replaced by an effective material (EM). EMs are based on physical observable values, such as eddy current losses (ECLs) and reactive powers (RPs), and are calculated a priori using a meaningful part of the heterogeneous structure. An EM is derived from this cell problem using the physical variables, which is then used in a simulation with a homogenized core, i.e., without taking the periodic structure into account. The results of this simulation can then be used to determine the ECLs and RP of the machine or transformer with a laminated core. Furthermore, the averaged ECL and RP density distributions can also be determined. For this work, a nonlinear magnetic material is used for the simulation of a single-phase transformer. Compared with the reference simulations of the numerical example with a laminated core, the novel approach with the homogenized core and the EM can dramatically reduce the demands on the computer structure, whereby the ECLs as well as the RP and the corresponding averaged distributions are very well approximated.

***Index Terms*— Eddy currents, effective material, finite-element method, homogenization method, iron sheets, nonlinear material, time-domain simulation.**

I. Introduction

THIS work deals with the homogenization of nonlinear magnetic materials in the context of an eddy current problem (ECP) in electrical machines or transformers with laminated cores by an effective material (EM). Laminated cores are composed of insulated iron sheets in order to minimize the eddy current losses (ECLs).

The theoretical background for non-oriented electrical steel sheets modeled by the parametric magnetodynamic model for hysteresis is discussed in [1]. The EM theory is a well-known homogenization technique [2] for heterogeneous structures, such as laminated iron cores [3].

Most homogenization techniques preserve the physical nature of the problem [2]. For instance, an early study of the ECLs in a single nonlinear sheet in one and two dimensions is shown in [4]. A time-domain homogenization method of a nonlinear laminated iron core is derived in [5] and applied in a time-domain simulation. A homogenization technique with an anisotropic material tensor for low frequencies is derived in [6]. A rate-dependent finite-difference homogenization approach, including hysteretic losses, is presented in [7] for a 1-D example. Investigations of losses, using the Bertotti model [8], in amorphous core transformers with an anisotropic permeability are shown in [9]. A homogenization approach for laminated ferromagnetic cores based on the heterogeneous multiscale method for nonlinear reversible and nonlinear irreversible materials, in which upscaling and downscaling steps are necessary to compute the material relation between mesoscale and macroscale, is given in [10]. An investigation of an equivalent circuit approach to model laminated cores is presented in [11]. Comparisons of different approximation formulas to compute ECL and equivalent conductivities are shown in [12].

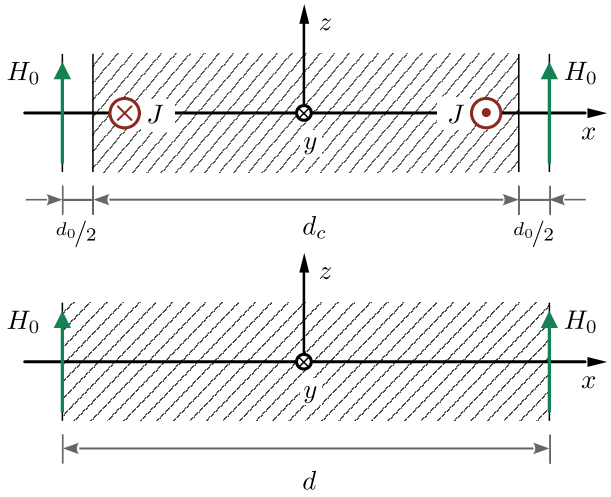

Fig. 1. Single sheet for the reference CP (top) and the homogenized CP (bottom) of total width $d = d_0 + d_c$.

In this work, an EM in the form of a complex-valued nonlinear permeability $\mu_{\text{eff}}(|\boldsymbol{H}|)$ is used in a static magnetic field problem (SMFP) instead of an ECP, while retaining the ECL and the reactive power (RP) of the original ECP. Using an EM, it is neither necessary to use a time-stepping scheme [4], [5], [6], [7], [9], [10], [11], [12], [13], [14], [15], nor is it necessary to use a harmonic balance method [15], [16]. Furthermore, the novel method using the EM allows the laminated core in the 3-D problem to be considered as a bulk domain. These two advantages enable an enormous reduction in computational costs, especially in non-linear 3-D cases, while maintaining the accuracy.

In Section II, the formulation of an ECP is derived using the finite-element method (FEM) and applied to the 1-D cell problem (CP). In comparison with [3], the solution is based not

Manuscript received 19 April 2024; revised 5 July 2024 and 7 August 2024; accepted 15 August 2024. Date of publication 21 August 2024; date of current version 26 September 2024. Corresponding author: V. Hanser (e-mail: valentin.hanser@tuwien.ac.at).

Color versions of one or more figures in this article are available at https://doi.org/10.1109/TMAG.2024.3447126.

Digital Object Identifier 10.1109/TMAG.2024.3447126

only on the fundamental frequency of the occurring fields, but also takes into account harmonics of the fields using a time-stepping method. Using the calculated ECL and RP of the reference and the homogenized CP, an effective permeability $\mu_{\text{eff}}(|\boldsymbol{H}|)$, which is complex valued, is defined. In comparison with a 3-D reference simulation with a laminated core, shown in Section III, the EM is used in an SMFP, see Section IV. In the simulation using the EM, the same quantities, namely, the ECL and the RP in the steady state, can be approximated accurately while reducing the computational costs enormously. In Section V, the local distributions of the ECL and the RP are determined and compared with the corresponding distributions in the reference problem. Numerical examples in Section VI, with sinusoidal and triangular excitation, for a variety of geometry settings demonstrate the high accuracy and the enormous reduction of computational costs of the novel approach. Finally, the conclusions are given in Section VII.

II. Cell Problem

The boundary value problem (BVP) of the 1-D CP, see Fig. 1, is formulated to calculate the effective permeability $\mu_{\text{eff}}(|\boldsymbol{H}|)$. A single sheet of total width $d = d_c + d_0$, with the width d_c of the conducting sheet and the total width d_0 of the insulating layer, is considered, which is excited by $\boldsymbol{H}_0$ in tangential $\boldsymbol{e}_z$-direction. The resulting eddy currents $\boldsymbol{J}$ are oriented in the $\boldsymbol{e}_y$-direction.

A. Eddy Current Problem

The BVP of the ECP is based on Maxwell's equations

$$\nabla \times \boldsymbol{H} = \boldsymbol{J}, \quad \nabla \cdot \boldsymbol{B} = 0 \quad \text{and} \quad \nabla \times \boldsymbol{E} = -\partial_t \boldsymbol{B} \tag{1}$$

where $\boldsymbol{H}$ is the magnetic field strength, $\boldsymbol{B}$ the magnetic flux density, $\boldsymbol{E}$ the electric field, and $\boldsymbol{J}$ the eddy current density. With the electric resistivity ρ and the magnetic permeability μ, the constitutive relations are $\boldsymbol{E} = \rho \boldsymbol{J}$ and $\boldsymbol{B} = \mu \boldsymbol{H}$. On this base, the BVP

$$\nabla \times \rho \nabla \times \boldsymbol{H} + \partial_t(\mu \boldsymbol{H}) = \boldsymbol{0} \qquad \text{in } \Omega \tag{2a}$$

$$\boldsymbol{H} \times \boldsymbol{n} = \boldsymbol{K}_0 \qquad \text{on } \Gamma_H \tag{2b}$$

where the excitation of the problem is given by Dirichlet boundary values on the boundaries $\Gamma_H \subset \partial\Omega$, is derived.

B. Weak Form

For the nonlinear 1-D reference CP, see Fig. 1 (top), a single-component magnetic field strength $\boldsymbol{H} = H(x)\boldsymbol{e}_z$ with the corresponding eddy current density $\boldsymbol{J} = -\partial_x H(x)\boldsymbol{e}_y$ is applied. With an implicit Euler time-stepping scheme $\partial_t H \approx (1/\Delta t)(H - \widehat{H})$, where the hat symbol denotes the values of the previous time instant and Δt denotes the time step, the BVP reads as follows:

Find $H \in \mathrm{V}_D := \{H \in \mathcal{U} : H = H_0(t) \text{ on } \partial\mathcal{I}\}$, such that

$$\int_{\mathcal{I}_c} \left(\Delta t \rho_c \partial_x H \partial_x H' + \mu(|H|) H H'\right) \mathrm{d}x = \int_{\mathcal{I}_c} \widehat{\mu}\left(|\widehat{H}|\right) \widehat{H} H' \,\mathrm{d}x \quad \text{in } \mathcal{I}_c \tag{3a}$$

and

$$\int_{\mathcal{I}_0} \left(\Delta t \rho_0 \partial_x H \partial_x H' + \mu_0 H H'\right) \mathrm{d}x = \int_{\mathcal{I}_0} \mu_0 \widehat{H} H' \,\mathrm{d}x \quad \text{in } \mathcal{I}_0 \tag{3b}$$

for all $H' \in \mathrm{V}_0$, where $\mathcal{I} = [-d/2, d/2]$, $\mathcal{I}_c = [-d_c/2, d_c/2]$, $\mathcal{I}_0 = \mathcal{I} \backslash \mathcal{I}_c$, $\mathcal{U} \subset H^1(\mathcal{I})$, and ρ_0 is a sufficiently large electric resistivity in air. The test functions are denoted by the prime symbol, and the excitation is given by the time-dependent Dirichlet boundary values H_0. The nonlinear permeability $\mu(|H|)$ is treated according to [13].

C. ECLs and RP

For the calculation of the effective permeability μ_{eff}, the ECLs P and the RP Q are required.

1) Reference Model: In the reference CP, the instantaneous values of the ECL and the RP

$$p(t) = \frac{1}{d} \int_{I_c} E \; J \,\mathrm{d}x \tag{4a}$$

$$q(t) = \frac{1}{d} \int_{I} \frac{1}{2T} H \; B \,\mathrm{d}x \tag{4b}$$

respectively, where the time period $T = 1/f$ is the inverse of the frequency f, are calculated in every time instant. A set of instantaneous ECLs and RPs is shown in Fig. 2. The curves are based on the measured BH curve in Fig. 3 (blue) and are obtained by sinusoidal excitation of different amplitudes H_p. The twin peaks in the instantaneous ECL are a consequence of the convex–concave nature of the nonlinear BH curve. The nonlinear behavior is also visible in the non-sinusoidal curves of the RP. In the steady state, i.e., $H(t') = H(t' + T)$, the average ECL and average RP

$$P = \frac{1}{T} \int_{t'}^{t'+T} p(t) \,\mathrm{d}t \tag{5a}$$

$$Q = \frac{1}{T} \int_{t'}^{t'+T} q(t) \,\mathrm{d}t \tag{5b}$$

are considered, respectively. Consequently, the apparent power (AP)

$$\underline{S}_{\text{ref}} = P + j\,Q \tag{6}$$

where j denotes the imaginary unit and the underline denotes complex valued, is determined.

2) Homogenized Model: In the homogenized problem, an SMFP is considered. In the specific case of the homogenized 1-D CP, see Fig. 1 (bottom), the magnetic field strength $\underline{H}(x) = H_0$ is constant. With the constitutive relation $\underline{B} = \mu_{\text{eff}} \underline{H}$, the AP

$$\underline{S}_{\text{eff}} = \frac{j}{2Td} \mu^*_{\text{eff}} \int_I \underline{H} \; \underline{H}^* \,\mathrm{d}x = j \frac{H_0^2}{2T} \mu^*_{\text{eff}} \tag{7}$$

where the superscript * indicates the complex conjugate, is determined analytically.

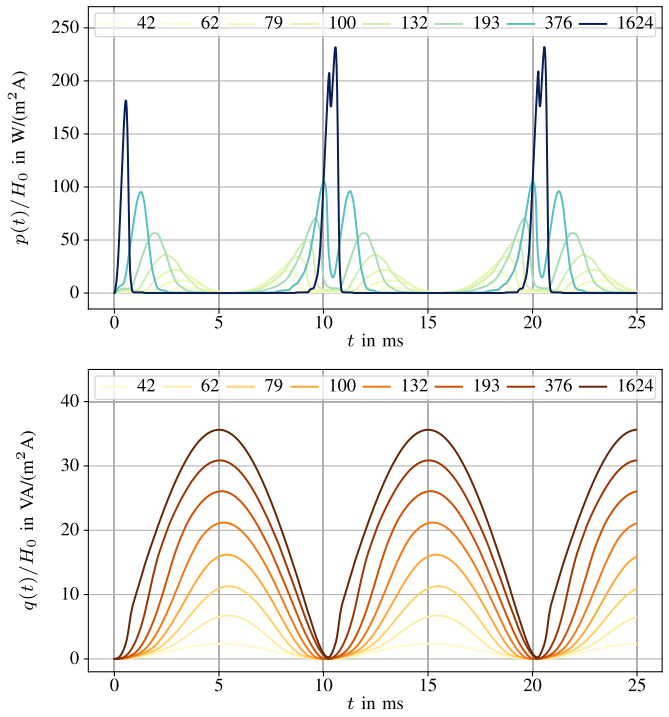

Fig. 2. Instantaneous values of the ECLs $p(t)$ (top) and the RP $q(t)$ (bottom) over time for a nonlinear material with $H_0 = H_p \sin(\omega t)$, $H_p \in (0, 1624]$ A/m, and $f = 50$ Hz.

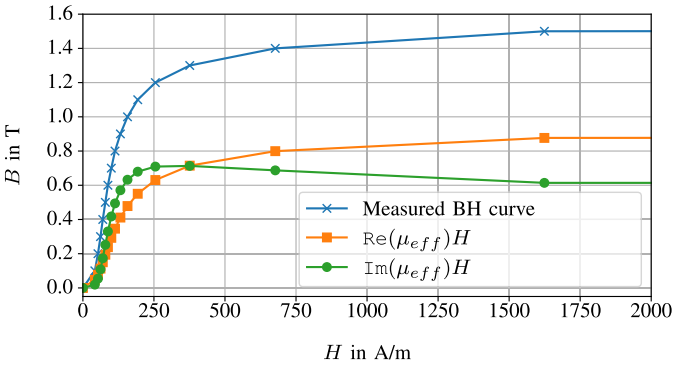

Fig. 3. *BH* curves of an effective permeability μ_{eff} with an $f = 50$ Hz sinusoidal excitation.

D. Calculation of the EM

The purpose of introducing the EM in an equivalent problem with a homogenized core is to reproduce the ECL and the RP, i.e.,

$$\underline{S}_{\text{ref}} = \underline{S}_{\text{eff}} \quad \text{or} \quad P + jQ = j\frac{H_0^2}{2T}\mu_{\text{eff}}^* \tag{8}$$

without the requirement of modeling the individual sheets. Therefore, the effective permeability

$$\mu_{\text{eff}}(H_0) = \frac{2T}{H_0^2}(jP + Q) \tag{9}$$

is derived. A resulting effective permeability based on a measured *BH* curve (blue) for the reference problem with sinusoidal excitation and a frequency $f = 50$ Hz is shown as *BH* curves in Fig. 3.

III. Three-Dimensional Reference Problem

In the 3-D reference problem, each sheet of the laminated core is modeled in the mesh, see Fig. 4 (top). Using the $\boldsymbol{T}$, Φ-Φ formulation, the nonlinear BVP

$$\begin{aligned}
\nabla \times (\rho_c \nabla \times \boldsymbol{T}) + \partial_t(\mu(\boldsymbol{T} - \nabla\Phi)) \\
\quad = -\partial_t(\mu \boldsymbol{H}_{\text{BS}}) && \text{in } \Omega_c && \text{(10a)}\\
\nabla \cdot (\mu \boldsymbol{T} - \mu\nabla\Phi) = -\nabla \cdot (\mu \boldsymbol{H}_{\text{BS}}) && \text{in } \Omega_c && \text{(10b)}\\
-\nabla \cdot (\mu_0 \nabla\Phi) = -\nabla \cdot (\mu_0 \boldsymbol{H}_{\text{BS}}) && \text{in } \Omega_0 && \text{(10c)}\\
\boldsymbol{T} \times \boldsymbol{n} = \boldsymbol{0} && \text{on } \Gamma_{0c} \cup \Gamma_{H_c} && \text{(10d)}\\
\Phi = 0 && \text{on } \Gamma_H && \text{(10e)}
\end{aligned}$$

with the current vector potential $\boldsymbol{T}$, the magnetic scalar potential Φ, and a known Biot–Savart field $\boldsymbol{H}_{\text{BS}}$, is applied. The interface between conducting domain and non-conducting domain is denoted by Γ_{0c}, and the far boundary and the boundaries in the $x = 0$ plane and the $y = 0$ plane are denoted by $\Gamma_H = \Gamma_{H_0} \cup \Gamma_{H_c} \subset \partial\Omega$. The solution of the BVP yields the magnetic field strength $\boldsymbol{H} = \boldsymbol{T} - \nabla\Phi + \boldsymbol{H}_{\text{BS}}$ and the current density $\boldsymbol{J} = \nabla \times \boldsymbol{T} + \boldsymbol{J}_{\text{BS}}$, where $\boldsymbol{J}_{\text{BS}}$ denotes the known current density in the exciting coils [17].

A. Weak Form

Using the notation of (3) for the implicit Euler time-stepping scheme and the test functions, the weak formulation reads as follows.

Find $(\boldsymbol{T}, \Phi) \in V_D := \{(\boldsymbol{T}, \Phi) : \boldsymbol{T} \in \mathcal{U},\ \Phi \in \mathcal{V}$ and $\boldsymbol{T} \times \boldsymbol{n} = \boldsymbol{0}$ on $\Gamma_{0c} \cup \Gamma_{H_c},\ \Phi = 0$ on $\Gamma_H\}$, such that

$$\begin{aligned}
&\Delta t \int_{\Omega_c} \rho \nabla \times \boldsymbol{T} \cdot \nabla \times \boldsymbol{T}' \, \mathrm{d}\Omega \\
&\quad + \int_{\Omega_c} \mu(|\boldsymbol{H}|)(\boldsymbol{T} - \nabla\Phi) \cdot \left(\boldsymbol{T}' - \nabla\Phi'\right) \mathrm{d}\Omega \\
&= -\int_{\Omega_c} \left(\mu(|\boldsymbol{H}|)\boldsymbol{H}_{\text{BS}} - \widehat{\mu}\left(|\widehat{\boldsymbol{H}}|\right)\widehat{\boldsymbol{H}}_{\text{BS}}\right) \cdot \left(\boldsymbol{T}' - \nabla\Phi'\right) \mathrm{d}\Omega \\
&\quad + \int_{\Omega_c} \widehat{\mu}\left(|\widehat{\boldsymbol{H}}|\right)\left(\widehat{\boldsymbol{T}} - \nabla\widehat{\Phi}\right) \cdot \left(\boldsymbol{T}' - \nabla\Phi'\right) \mathrm{d}\Omega \quad \text{in } \Omega_c \qquad \text{(11a)}
\end{aligned}$$

and

$$\begin{aligned}
\int_{\Omega_0} \mu_0 \nabla\Phi \cdot \nabla\Phi' \, \mathrm{d}\Omega = \int_{\Omega_0} \mu_0 \left(\boldsymbol{H}_{\text{BS}} - \widehat{\boldsymbol{H}}_{\text{BS}}\right) \cdot \nabla\Phi' \, \mathrm{d}\Omega \\
+ \int_{\Omega_0} \mu_0 \nabla\widehat{\Phi} \cdot \nabla\Phi' \, \mathrm{d}\Omega \text{ in } \Omega_0 \qquad \text{(11b)}
\end{aligned}$$

for all $(\boldsymbol{T}', \Phi') \in V_0$, where $\mathcal{U}$ and $\mathcal{V}$ are finite-element subspaces of $H(\text{curl}, \Omega_c)$ and $H^1(\Omega)$, respectively [18].

B. Calculation of ECLs and RP

Analogously to (6), the ECLs and the RP in the steady state are combined to the AP. Therefore, the instantaneous values of the ECL and the RP

$$p(t) = \frac{1}{|\Omega_m|} \int_{\Omega_c} \boldsymbol{E} \cdot \boldsymbol{J} \, \mathrm{d}\Omega \tag{12a}$$

$$q(t) = \frac{1}{|\Omega_m|} \int_{\Omega_m} \frac{1}{2T} \boldsymbol{H} \cdot \boldsymbol{B} \, \mathrm{d}\Omega \tag{12b}$$

where Ω_m denotes the domain of the laminated core, i.e., the sheets including the insulating layers and $|\Omega_m|$ its volume, are used to calculate the averaged ECL P and the averaged RP Q, see [5].

IV. Problem With a Homogenized Core and EM

In order to approximate the averaged ECLs and the averaged RP of the reference problem in Section III, the complex valued equivalent SMFP

$$-\nabla\cdot\left(\mu_{\text{eff}}\nabla\underline{\Phi}\right) = -\nabla\cdot\left(\mu_{\text{eff}}\boldsymbol{H}_{\text{BS}}\right) \quad \text{in } \Omega_m \tag{13a}$$

$$-\nabla\cdot\left(\mu_0\nabla\underline{\Phi}\right) = -\nabla\cdot\left(\mu_0\boldsymbol{H}_{\text{BS}}\right) \quad \text{in } \Omega_0 \tag{13b}$$

$$\Phi = 0 \quad \text{on } \Gamma_H \tag{13c}$$

with the nonlinear EM μ_{eff} is solved; see Fig. 4 (bottom).

A. Weak Form

The weak form of the equivalent BVP reads as follows. Find $\underline{\Phi}\in \mathrm{V}_D(\Omega)$:$\{\underline{\Phi}\in\mathcal{U}$:$\underline{\Phi}=0$ on $\Gamma_H\}$, such that

$$\int_{\Omega_m}\mu_{\text{eff}}\left(|\underline{\boldsymbol{H}}|\right)\nabla\underline{\Phi}\cdot\nabla\underline{\Phi}'\,\mathrm{d}\Omega = \int_{\Omega_m}\mu_{\text{eff}}\left(|\underline{\boldsymbol{H}}|\right)\boldsymbol{H}_{\text{BS}}\cdot\nabla\underline{\Phi}'\,\mathrm{d}\Omega \quad \text{in } \Omega_m \tag{14a}$$

and

$$\int_{\Omega_0}\mu_0\nabla\underline{\Phi}\cdot\nabla\underline{\Phi}'\,\mathrm{d}\Omega = \int_{\Omega_0}\mu_0\boldsymbol{H}_{\text{BS}}\cdot\nabla\underline{\Phi}'\,\mathrm{d}\Omega \quad \text{in } \Omega_0 \tag{14b}$$

for all $\underline{\Phi}'\in \mathrm{V}_0$ and $\mathcal{U}\subset \mathrm{H}^1(\Omega)$.

B. Reconstruction of ECL and RP

With the magnetic field strength $\underline{\boldsymbol{H}} = -\nabla\underline{\Phi}+\boldsymbol{H}_{\text{BS}}$ and the magnetic flux density $\underline{\boldsymbol{B}}=\mu_{\text{eff}}\underline{\boldsymbol{H}}$, the effective AP of the homogenized core Ω_m

$$\underline{S}_{\text{eff}} = \frac{j}{|\Omega_m|}\int_{\Omega_m}\frac{1}{2T}\underline{\boldsymbol{H}}\cdot\underline{\boldsymbol{B}}^*\,\mathrm{d}\Omega \tag{15}$$

is calculated. To reconstruct the ECL and the RP, the AP is separated by

$$\underline{S}_{\text{eff}} = \widetilde{P} + j\,\widetilde{Q} \tag{16}$$

into the approximated ECL $\widetilde{P}=\mathrm{Re}(\underline{S}_{\text{eff}})$ and the approximated RP $\widetilde{Q}=\mathrm{Im}(\underline{S}_{\text{eff}})$, where the tilde symbol indicates values based on the EM.

V. Comparison of the Loss Distributions

The ECLs and the RP in the reference problem (6) and the approximated ECL and RP in the homogenized problem (16) are equivalent. Hence, the local ECL and RP distributions of the reference problem averaged over one period in time and averaged over every ith sheet in normal direction of the sheet, here the z-direction,

$$\overline{p}_i(x,y) = \frac{1}{d}\int_{d_{c,i}}\frac{1}{T}\int_{t'}^{t'+T}\boldsymbol{E}\cdot\boldsymbol{J}\,\mathrm{d}t\mathrm{d}z \tag{17a}$$

$$\overline{q}_i(x,y) = \frac{1}{d}\int_{d_i}\frac{1}{T}\int_{t'}^{t'+T}\frac{1}{2T}\boldsymbol{H}\cdot\boldsymbol{B}\,\mathrm{d}t\mathrm{d}z \tag{17b}$$

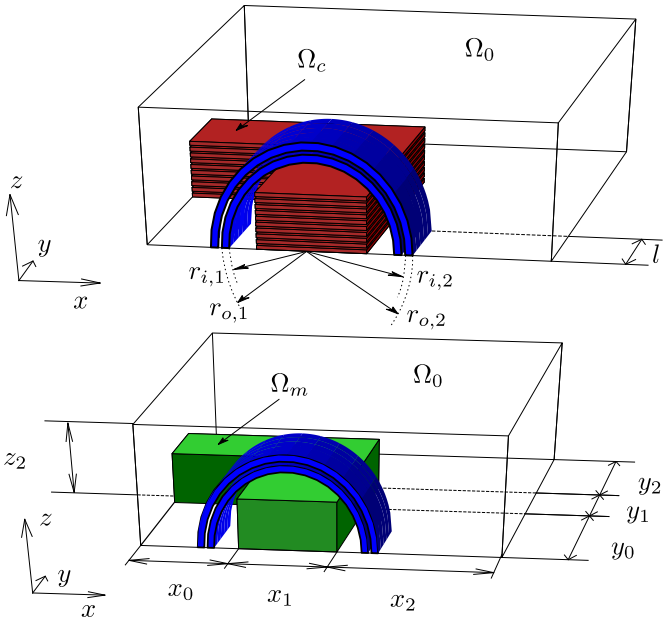

Fig. 4. Geometry with exciting coils (blue) for the reference problem (top) with individual sheets (red) and homogenized problem (bottom) with a bulk medium (green); symmetries are utilized.

are equivalent to the corresponding fields in the homogenized problem, respectively.

Based on the solution of the homogenized problem, the averaged AP distribution in the ith sheet

$$\widetilde{s}_i(x,y) = \frac{j}{d}\int_{d_i}\frac{1}{2T}\underline{\boldsymbol{H}}\cdot\underline{\boldsymbol{B}}^*\,\mathrm{d}z \tag{18}$$

is determined, which can be separated into the ECL and RP distribution

$$\widetilde{p}_i(x,y) = \mathrm{Re}\left(\widetilde{s}_i(x,y)\right) \tag{19a}$$

$$\widetilde{q}_i(x,y) = \mathrm{Im}\left(\widetilde{s}_i(x,y)\right) \tag{19b}$$

respectively.

VI. Numerical Example

A single-phase transformer is used as a numerical example. The geometry of the laminated iron core is shown in Fig. 4 (top), where all symmetries are utilized. The dimensions $x_0 = 156$ mm, $x_1 = 94$ mm, $x_2 = 334.5$ mm, $y_0 = 250$ mm, $y_1 = 94$ mm, $y_2 = 334.5$ mm, and $z_2 = 334.5$ mm are used. The thickness of one conducting sheet is $d_c = 0.5$ mm, the filling factor $k_F = d_c/(d_c+d_0) = 0.95$, and the core is composed of 20 or 184 sheets. In order to emphasize the additional increase in efficiency and to enable a comparison with the results in [14] and [19], the reference simulations with 184 sheets were carried out. The excitation of the problem is considered by the Biot–Savart field of four symmetric cylindrical coils with 60 turns each. The inner and outer radii of the coils are, respectively, selected as $r_{i,1} = 81$ mm, $r_{o,1} = 84$ mm, $r_{i,2} = 88$ mm, and $r_{o,2} = 91$ mm, and the length of the coil as $l = 192$ mm. The electric conductivity of iron is selected as $\sigma_c = \rho_c^{-1} = 2.08\cdot 10^6$ S/m, and the frequency as $f = 50$ Hz. The arrangement of the core with the coils exhibits

TABLE I
ECLS AND RP (SINUSOIDAL EXCITATION)

I_0	FEM P	FEM Q	EM P	EM Q	ε_P	ε_Q
A	W/m^3	VA/m^3	W/m^3	VA/m^3	%	%
20 sheets						
0.5	203.9	199.8	207.8	195.3	-1.9	2.2
1.0	1,674.3	1,231.5	1,638.0	1,193.1	2.2	3.1
2.0	4,312.5	3,853.6	4,217.9	3,765.6	2.2	2.3
3.0	6,509.8	6,557.3	6,354.6	6,430.8	2.4	1.9
184 sheets						
0.5	203.5	199.6	207.1	194.8	-1.8	2.4
1.0	1,676.1	1,231.5	1,635.7	1,191.7	2.4	3.2
2.0	4,340.8	3,855.7	4,235.4	3,773.7	2.4	2.1
3.0	6,565.9	6,562.8	6,403.9	6,433.1	2.5	2.0
$\boldsymbol{A}$-Formulation, 20 sheets						
1.0	1,610.8	1,198.9				

TABLE II
COMPUTATIONAL COSTS (SINUSOIDAL EXCITATION)

I_0	FEM t_{sim}	FEM N_{dof}	EM t_{sim}	EM N_{dof}	speedup	ratio N_{dof}
A	s	10^3	s	10^3	10^3	
20 sheets						
0.5	13,407	324.3	1.4	6.7	9.8	48.3
1.0	13,702	"	0.9	"	14.7	"
2.0	13,663	"	1.2	"	11.8	"
3.0	14,032	"	1.2	"	11.7	"
184 sheets						
0.5	115,447	2,937	1.6	6.7	74.2	437.1
1.0	116,072	"	1.3	"	92.9	"
2.0	117,924	"	1.7	"	71.4	"
3.0	118,547	"	2.0	"	59.7	"
$\boldsymbol{A}$-Formulation, 20 sheets						
1.0	39,785	134.8				

three planes of symmetry. Handmade structured hexahedral finite-element meshes are used. The same discretization by finite elements in the xy plane are used for the reference model and the model with the homogenized core to ensure a fair comparison. One period of time is discretized in 200 instants. The reference solution is computed to verify the results obtained by the approach using the EM and is verified against simulations with an $\boldsymbol{A}$-formulation [15]. All simulations are implemented using Netgen/NGSolve [20].

A. Sinusoidal Excitation

Simulations with different peak values of the sinusoidal impressed current I_0 are carried out. A comparison of the ECLs and the RP between the reference problem and the approach using the EM is summarized in Table I, where a relative error $\varepsilon_G = (G_{\mathrm{EM}} - G_{\mathrm{FEM}})/(G_{\mathrm{FEM}}) \cdot 100\%$ for $G \in \{P, Q\}$ is calculated. The results show errors of the novel homogenization method with the EM of around 3% for all setups. The computational costs, given by the calculation time t_{sim} and the number of unknowns N_{dof}, and the speedup

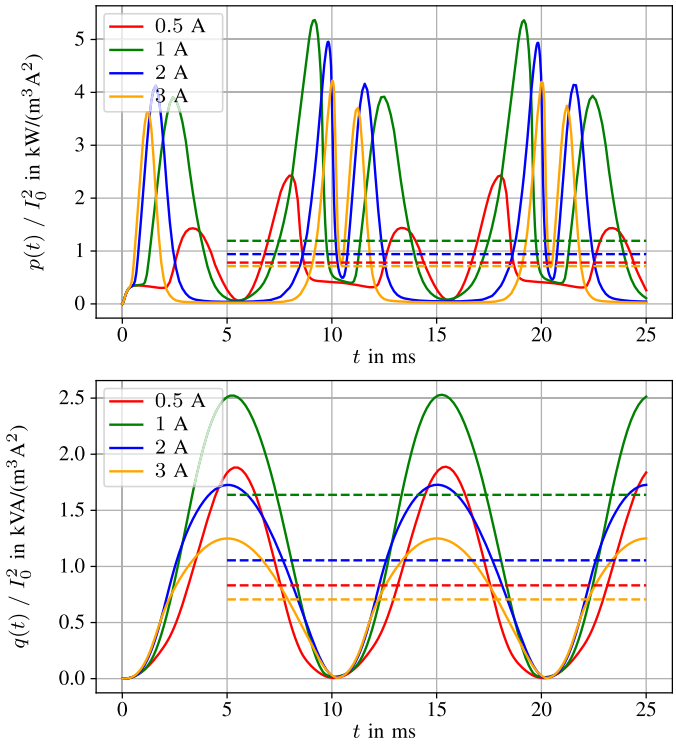

Fig. 5. ECLs (top) and RP (bottom) scaled by I_0^2 over time for the 3-D problem, excited with $I_0 \in \{0.5, 1, 2, 3\}$ A. Solid lines for the reference problem, and dashed lines for the homogenized problem.

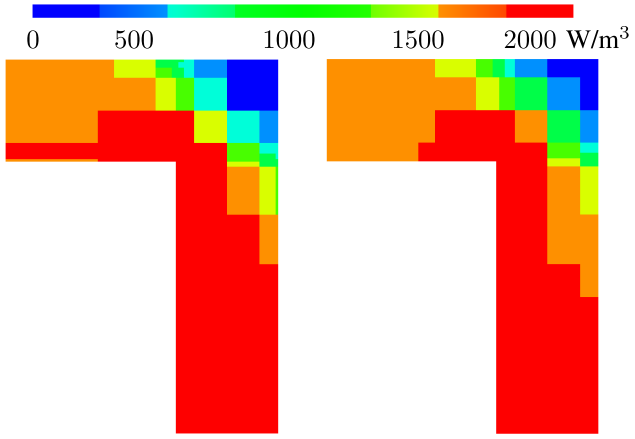

Fig. 6. Distribution of the ECLs $\overline{p}_{20}(x, y)$ (17a) in the reference problem (left) and $\widetilde{p}_{20}(x, y)$ (19a) with the EM (right) model in the top most sheet with 20 sheets and $I_0 = 1$ A.

$t_{\mathrm{sim,FEM}}/t_{\mathrm{sim,EM}}$ of all simulations are shown in Table II. The speedup of the approach using the EM is around 10 000 for 20 sheets and around 70 000 for 184 sheets while retaining a high accuracy of the ECL and the RP. In comparison, the mixed-multiscale FEM presented in [14] and [19] achieves only a speedup of around 10 for the given setups and is, therefore, much slower. The instantaneous value of the ECL and the RP (solid lines) and the corresponding approximated ECL and the approximated RP (dashed lines) for 20 sheets and different peak values of the exciting currents I_0 are shown in Fig. 5. Since the same BH curve is used as in the CP, twin

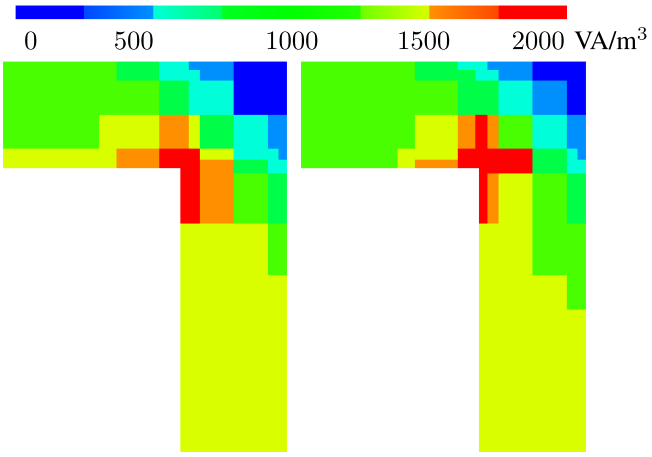

Fig. 7. Distribution of the RP $\overline{q}_{20}(x, y)$ (17b) in the reference problem (left) and $\widetilde{q}_{20}(x, y)$ (19b) with the EM (right) model in the top most sheet with 20 sheets and $I_0 = 1$ A.

TABLE III
ECLs AND RP (DIFFERENT FILLING FACTORS)

k_F	FEM P	FEM Q	EM P	EM Q	ε_P	ε_Q
	W/m^3	VA/m^3	W/m^3	VA/m^3	%	%
20 sheets						
0.95	1,674.3	1,231.5	1,638.0	1,193.1	2.2	3.1
0.9	1,586.4	1,166.7	1,551.7	1,130.3	2.2	3.1
0.8	1,410.3	1,037.0	1,379.3	1,004.7	2.2	3.1
0.5	881.1	648.1	862.1	628.1	2.2	3.1

peaks can also be recognized in the instantaneous ECL, and non-sinusoidal curves can be seen in the instantaneous RP.

The distributions of the time and sheet averaged ECL (17a) and (19a) and RP (17b) and (19b) are shown in Figs. 6 and 7, respectively.

B. Influence of the Filling Factor

Simulations with different filling factors $k_F \in \{0.5, 0.8, 0.9\}$, 20 sheets, and a peak value of the exciting current of $I_0 = 1$ A are carried out. As shown in Table III, the simulations result in the errors $\varepsilon_p = 2.2\%$ and $\varepsilon_Q = 3.1\%$ for the ECL and the RP, respectively, which are the same as with the filling factor of $k_F = 0.95$.

C. Non-Sinusoidal Excitation

In the previous examples, a sinusoidal excitation H_0 was selected. In real scenarios, higher harmonics also occur in addition to the fundamental frequency. For simulations with higher harmonics, the CP has to be excited by the corresponding time-dependent excitation H_0. The obtained EM is then used according to Section IV to solve the 3-D approximation problem. As an example, the triangular excitation $H_0 = H_p \text{triag}(\omega t)$, shown in Fig. 8, was selected as a non-sinusoidal one. The resulting EM is shown as *BH* curves in Fig. 9. The ECL and the RP of the 3-D problem with 20 sheets under triangular excitation are compared in Table IV.

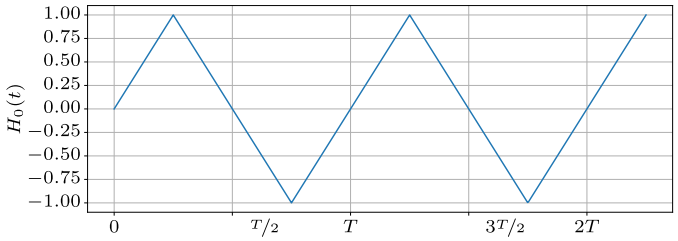

Fig. 8. Triangular excitation $H_0(t) = \text{triag}(\omega t)$ as an example of a non-sinusoidal one.

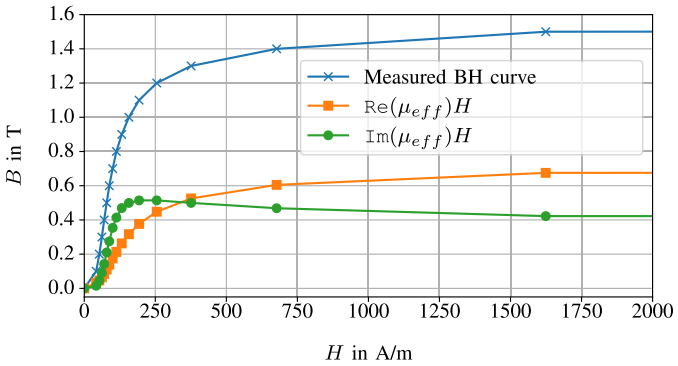

Fig. 9. *BH* curves of an effective permeability μ_{eff} with an $f = 50$ Hz triangular excitation.

TABLE IV
ECLs AND RP (NON-SINUSOIDAL EXCITATION)

I_0	FEM P	FEM Q	EM P	EM Q	ε_P	ε_Q
A	W/m^3	VA/m^3	W/m^3	VA/m^3	%	%
20 sheets						
0.5	164.1	113.7	172.6	111.8	-5.1	1.7
1.0	1,355.6	786.6	1,343.2	760.9	0.9	3.3
2.0	3,103.7	2,747.1	3,071.8	2,672.9	1.0	2.7
3.0	4,531.1	4,840.3	4,474.3	4,729.5	1.3	2.3

VII. CONCLUSION

A novel method for accurately calculating the ECLs and RP in laminated magnetic cores through the use of an EM was introduced. This method significantly reduces computational costs while maintaining high accuracy. A complex-valued SMFP for the homogenized core was formulated, which eliminates, on the one hand, the need for time-stepping or harmonic balance methods and, on the other hand, the need to model each individual sheet separately.

Simulations of 3-D cores demonstrated that the EM approach yields robust results with errors around 3% for both ECL and RP across various setups, including different saturation levels of the material with sinusoidal and triangular excitation currents, different filling factors and different numbers of sheets. The method also shows exceptional computational efficiency, with a speedup of approximately 10 000 for 20 sheets and around 70 000 for 184 sheets when compared with conventional FEM simulations.

The local distributions of ECL and RP were found to be in excellent agreement with the corresponding distributions in the reference problems, confirming the method's accuracy and applicability.

In conclusion, the proposed EM-based homogenization technique offers a powerful and efficient tool for analyzing magnetic cores in electrical machines and transformers. It enables substantial reductions in computational costs while delivering precise estimations of the ECL and the RP, making it highly beneficial to both research and industrial applications.

ACKNOWLEDGMENT

This research was funded in whole or in part by the Austrian Science Fund (FWF) grant DOI:10.55776/P36395. For open access purposes, the author has applied a CC BY public copyright license to any author accepted manuscript version arising from this submission.

REFERENCES

[1] M. Petrun and S. Steentjes, "Iron-loss and magnetization dynamics in non-oriented electrical steel: 1-D excitations up to high frequencies," *IEEE Access*, vol. 8, pp. 4568–4593, 2020.

[2] I. Tsukerman, "Computational electromagnetics: A miscellany," *J*, vol. 4, no. 4, pp. 881–896, Dec. 2021. [Online]. Available: https://www.mdpi.com/2571-8800/4/4/60

[3] M. Schöbinger, I. Tsukerman, and K. Hollaus, "Effective medium transformation: The case of eddy currents in laminated iron cores," *IEEE Trans. Magn.*, vol. 57, no. 11, pp. 1–6, Nov. 2021.

[4] J. Gyselinck, L. Vandevelde, J. Melkebeek, P. Dular, F. Henrotte, and W. Legros, "Calculation of eddy currents and associated losses in electrical steel laminations," *IEEE Trans. Magn.*, vol. 35, no. 3, pp. 1191–1194, May 1999.

[5] J. Gyselinck, R. V. Sabariego, and P. Dular, "A nonlinear time-domain homogenization technique for laminated iron cores in three-dimensional finite-element models," *IEEE Trans. Magn.*, vol. 42, no. 4, pp. 763–766, Apr. 2006.

[6] H. Kaimori, A. Kameari, and K. Fujiwara, "FEM computation of magnetic field and iron loss in laminated iron core using homogenization method," *IEEE Trans. Magn.*, vol. 43, no. 4, pp. 1405–1408, Apr. 2007.

[7] A. J. Bergqvist and S. G. Engdahl, "A homogenization procedure of field quantities in laminated electric steel," *IEEE Trans. Magn.*, vol. 37, no. 5, pp. 3329–3331, Sep. 2001.

[8] G. Bertotti, "General properties of power losses in soft ferromagnetic materials," *IEEE Trans. Magn.*, vol. 24, no. 1, pp. 621–630, Jan. 1988.

[9] T. Steinmetz, B. Cranganu-Cretu, and J. Smajic, "Investigations of no-load and load losses in amorphous core dry-type transformers," in *Proc. 19th Int. Conf. Elect. Mach. (ICEM)*, 2010, pp. 1–6.

[10] I. Niyonzima, R. V. Sabariego, P. Dular, F. Henrotte, and C. Geuzaine, "Computational homogenization for laminated ferromagnetic cores in magnetodynamics," *IEEE Trans. Magn.*, vol. 49, no. 5, pp. 2049–2052, May 2013.

[11] J. Smajic et al., "Computational and experimental investigation of distribution transformers under differential and common mode transient conditions," *IEEE Trans. Magn.*, vol. 53, no. 6, pp. 1–4, Jun. 2017.

[12] A. Bermudez, D. Gomez, and P. Salgado, "Eddy-current losses in laminated cores and the computation of an equivalent conductivity," *IEEE Trans. Magn.*, vol. 44, no. 12, pp. 4730–4738, Dec. 2008.

[13] O. Bíró and K. Preis, "Finite element calculation of time-periodic 3D eddy currents in nonlinear media," in *Proc. 3rd Jpn.-Hung. Joint Seminar Appl. Electromagn. Mater. Comput. Technolog.*, 1995, pp. 62–74.

[14] V. Hanser, M. Schöbinger, and K. Hollaus, "A mixed multiscale FEM for the eddy current problem with T,$\Phi - \Phi$ and vector hysteresis," *COMPEL Int. J. Comput. Math. Electr. Electron. Eng.*, vol. 41, no. 3, pp. 852–866, May 2022.

[15] K. Hollaus, "A MSFEM to simulate the eddy current problem in laminated iron cores in 3D," *COMPEL Int. J. Comput. Math. Electr. Electron. Eng.*, vol. 38, no. 5, pp. 1667–1682, Sep. 2019.

[16] S. Ausserhofer, O. Bíró, and K. Preis, "An efficient harmonic balance method for nonlinear eddy-current problems," *IEEE Trans. Magn.*, vol. 43, no. 4, pp. 1229–1232, Apr. 2007.

[17] O. Bíró, "Edge element formulations of eddy current problems," *Comput. Methods Appl. Mech. Eng.*, vol. 169, nos. 3–4, pp. 391–405, Feb. 1999.

[18] J. Schöberl and S. Zaglmayr, "High order Nédélec elements with local complete sequence properties," *COMPEL Int. J. Comput. Math. Electr. Electron. Eng.*, vol. 24, no. 2, pp. 374–384, Jun. 2005.

[19] K. Hollaus and M. Schöbinger, "A mixed multiscale FEM for the eddy-current problem with T, F–F in laminated conducting media," *IEEE Trans. Magn.*, vol. 56, no. 4, pp. 1–4, Apr. 2020.

[20] J. Schöberl. *Netgen/NGSolve*. Accessed: May 14, 2024. [Online]. Available: ngsolve.org